RESEARCH PAPERS

# Focusing transform-based direction-of-arrival method exploiting multi-cycle frequencies

HUANG Zhitao*, JIANG Wenli and ZHOU Yiyu

(School of Electronic Science and Engineering, National University of Defense Technology, Changsha 410073, China)

Received October 29, 2004; revised December 28, 2004

**Abstract** When single cycle frequency is employed, the existing spectral correlation-signal subspace fitting (SC-SSF) algorithms usually contain two disadvantages: those single-cycle estimators cannot reach the best performance; it is inconvenient to be applied in practice since the right cycle frequency has to be selected. Based on the Jacobi-Anger expansion and the idea of focusing transform, a new approach exploiting multi-cycle frequencies of cyclostationary signal is discussed in this paper. Simulation results demonstrate the effectiveness of the new method.

**Keywords:** cyclostationary signal, direction-of-arrival, multi-cycle frequencies, focusing transform.

The existing direction-of-arrival (DOA) estimation methods that exploit the cyclostationarity property of the signal-of-interest (SOI), such as cyclic MUSIC (or cyclic ESPRIT) and SC-SSF (spectral correlation-signal subspace fitting), should be more appropriately referred to as single-cycle estimators, since only one cycle frequency is employed[1−5]. However, for most cyclostationary signals encountered in radar, sonar and communication systems, cycle frequencies are not always unique[6]. Thus, the existing cyclic DOA estimation methods have at least two disadvantages: those single-cycle estimators cannot achieve the best performance; it is inconvenient to be applied in practice since the right cycle frequency has to be selected. These disadvantages require that the cyclostationarity property of the SOI should be exactly known beforehand. To solve these problems, a new DOA estimation method exploiting multi-cycle frequencies is proposed in this paper.

## 1 Method

It is assumed that there are totally $C$ cycle frequencies $\{\alpha_i,\ i=1, \cdots, C\}$ about the SOI. The uniform linear array (ULA) consists of $2M+1$ sensors with the middle one as a reference, and $D$ is the sensor separation. The array signal model is exactly the same as that in Ref. [3], which can be rewritten as

$$\boldsymbol{R}_{\boldsymbol{x}}^{\alpha_i}(\tau) = \boldsymbol{A}(\alpha_i, \Theta)\boldsymbol{R}_{\boldsymbol{s}}^{\alpha_i}(\tau), \quad i = 1, 2, \cdots, C, \tag{1}$$

where $\boldsymbol{x}(t)=[x_1(t), x_2(t), \cdots, x_{2M+1}(t)]$ is the array output signal vector, $\boldsymbol{s}(t)=[s_1(t), s_2(t), \cdots, s_d(t)]$ is the received signal vector, $\boldsymbol{R}_{\boldsymbol{x}}^{\alpha_i}(\tau)$ and $\boldsymbol{R}_{\boldsymbol{s}}^{\alpha_i}(\tau)$ are the cyclic auto-correlation vectors of $\boldsymbol{x}$ and $\boldsymbol{s}$, respectively, $\boldsymbol{A}(\alpha)$ is the direction matrix, and $\Theta=\{\theta_1, \theta_2, \cdots, \theta_d\}$ is the direction vector arising from $d$ sources,

$$\boldsymbol{R}_{\boldsymbol{x}}^{\alpha_i}(\tau)=[R_{x_1}^{\alpha_i}(\tau), R_{x_2}^{\alpha_i}(\tau), \cdots, R_{x_{2M+1}}^{\alpha_i}(\tau)]^{\mathrm{T}}, \tag{2}$$

$$\boldsymbol{A}(\alpha_i, \Theta) = [a_1(\alpha_i, \theta_1), a_2(\alpha_i, \theta_2), \cdots, a_{d_{\alpha_i}}(\alpha_i, \theta_{d_{\alpha_i}})], \tag{3}$$

$$\boldsymbol{R}_{\boldsymbol{s}}^{\alpha_i}(\tau)=[R_{s_1}^{\alpha_i}(\tau), R_{s_2}^{\alpha_i}(\tau), \cdots, R_{s_{d_{\alpha_i}}}^{\alpha_i}(\tau)]^{\mathrm{T}}, \tag{4}$$

$$a_k(\alpha_i, \theta_k)=[\mathrm{e}^{-\mathrm{j}2\pi\alpha_i MD\sin\theta_k/c}, \cdots, \mathrm{e}^{\mathrm{j}2\pi\alpha_i MD\sin\theta_k/c}]^{\mathrm{T}}. \tag{5}$$

Here, we assume that only $d_{\alpha_i}$ sources are self correlated at the cycle frequency $\alpha_i$. The cyclic conjugate auto-correlation function $R_{x_i}^{\alpha}(\tau)$ of signal $x_i(t)$ is defined as[1]

$$R_{x_i}^{\alpha}(\tau) \triangleq \lim_{T\to\infty}\int_{-T/2}^{T/2} x_i(t+\tau/2) \cdot x_{x_1}^{*}(t-\tau/2)\mathrm{e}^{-\mathrm{j}2\pi\alpha t}\,\mathrm{d}t. \tag{6}$$

* To whom correspondence should be addressed. E-mail: talden@yahoo.com.cn

For each $\alpha_i$, a pseudodata matrix can be formed

$$\boldsymbol{X}(\alpha_i)=\begin{pmatrix} R^{\alpha}_{x_1}(0) & R^{\alpha}_{x_1}(T_s) & \cdots & R^{\alpha}_{x_1}(LT_s) \\ R^{\alpha}_{x_2}(0) & R^{\alpha}_{x_2}(T_s) & \cdots & R^{\alpha}_{x_2}(LT_s) \\ \vdots & \vdots & & \vdots \\ R^{\alpha}_{x_{2M+1}}(0) & R^{\alpha}_{x_{2M+1}}(T_s) & \cdots & R^{\alpha}_{x_{2M+1}}(LT_s) \end{pmatrix}, \tag{7}$$

where $\tau=0, T_s, \cdots, LT_s$; $T_s$ is the sampling period, and $(L+1)T_s$ is the data length. Pick SSF algorithm, e.g. MUSIC or ESPRIT, to estimate the directions of signals of interest (SOIs) based on this pseudodata matrix $\boldsymbol{X}(\alpha_i)$ or its sample covariance matrix $\boldsymbol{X}(\alpha_i)\boldsymbol{X}^{\mathrm{H}}(\alpha_i)$. In Ref. [3], such algorithms are called SC-SSF methods, e.g. SC-MUSIC or SC-ESPRIT. Now we consider how to estimate the DOAs of SOIs by exploiting the cyclostationary property at multi-cycle frequencies.

If there exists a matrix $\boldsymbol{T}(\alpha_i)$ which can change the direction matrix $\boldsymbol{A}(\alpha_i, \Theta)$ into $\boldsymbol{A}(\alpha_0, \Theta)$, namely

$$\boldsymbol{T}(\alpha_i)\boldsymbol{A}(\alpha_i, \Theta)=\boldsymbol{A}(\alpha_0, \Theta), \quad i=1, 2, \cdots, C, \tag{8}$$

$\boldsymbol{T}(\alpha_i)$ is referred to as the focusing matrix. Moreover, it follows directly from Eqs. (1) and (7) that we can obtain

$$\boldsymbol{T}(\alpha_i)\boldsymbol{R}^{\alpha_i}_{\boldsymbol{x}}(\tau)=\boldsymbol{A}(\alpha_0, \Theta)\boldsymbol{R}^{\alpha_i}_{\boldsymbol{s}}(\tau), \quad i=1, 2, \cdots, C, \tag{9}$$

and

$$\sum_{i=1}^{C}\boldsymbol{T}(\alpha_i)\boldsymbol{R}^{\alpha_i}_{\boldsymbol{x}}(\tau)=\boldsymbol{A}(\alpha_0, \Theta)\sum_{i=1}^{C}\boldsymbol{R}^{\alpha_i}_{\boldsymbol{s}}(\tau). \tag{10}$$

Let

$$\boldsymbol{R}_{\boldsymbol{x}}(\tau)\triangleq\sum_{i=1}^{C}\boldsymbol{T}(\alpha_i)\boldsymbol{R}^{\alpha_i}_{\boldsymbol{x}}(\tau), \tag{11}$$

$$\boldsymbol{R}_{\boldsymbol{s}}(\tau)\triangleq\sum_{i=1}^{C}\boldsymbol{R}^{\alpha_i}_{\boldsymbol{s}}(\tau), \tag{12}$$

it can be seen from Eq. (10) that

$$\boldsymbol{R}_{\boldsymbol{x}}(\tau)=\boldsymbol{A}(\alpha_0, \Theta)\boldsymbol{R}_{\boldsymbol{s}}(\tau). \tag{13}$$

Similarly, we can form a pseudodata matrix

$$\boldsymbol{X}=\begin{pmatrix} R_{x_1}(0) & R_{x_1}(T_s) & \cdots & R_{x_1}(LT_s) \\ R_{x_2}(0) & R_{x_2}(T_s) & \cdots & R_{x_2}(LT_s) \\ \vdots & \vdots & & \vdots \\ R_{x_{2M+1}}(0) & R_{x_{2M+1}}(T_s) & \cdots & R_{x_{2M+1}}(LT_s) \end{pmatrix}. \tag{14}$$

Pick SSF algorithm, e.g. MUSIC or ESPRIT, to estimate the DOAs of SOIs based on this sample covariance matrix $\overline{\boldsymbol{X}\boldsymbol{X}}^{\mathrm{H}}$. We shall call such algorithms MSC-SSF methods, e.g. MSC-MUSIC or MSC-ESPRIT, where MSC stands for multi-cycle spectral correlation. Now, the key problem is how to form the focusing matrix $\boldsymbol{T}(\alpha_i)$.

Just like Ref. [7], modal analysis techniques can be utilized to propose novel focusing matrix.

Through Jacobi-Anger expansion[7,8] we can obtain

$$\begin{aligned} \mathrm{e}^{\mathrm{j}\alpha x\sin\theta} &= \sum_{n=0}^{\infty}\mathrm{j}^n(2n+1)j_n(\alpha x)P_n(\sin\theta) \\ &= \sum_{n=0}^{N}\mathrm{j}^n(2n+1)j_n(\alpha x)P_n(\sin\theta) \\ &\quad + e(N), \end{aligned} \tag{15}$$

where $e(N)$ is the truncated error, $j_n(\cdot)$ is the spherical Bessel function, and $P_n(\cdot)$ is the Legendre function:

$$j_n(\alpha x)=\sqrt{\frac{\pi}{2\alpha x}}J_{n+0.5}(\alpha x), \tag{16}$$

$$P_n(\sin\theta)=\sum_{m=0}^{[l/2]}(-1)^m\frac{(2l-2m)!}{2^l m!(l-m)!(l-2m)!}\cdot(\sin\theta)^{l-2m}. \tag{17}$$

Here, $j_n(\cdot)$ is the first type of Bessel function, and $[\cdot]$ denotes the rounding operation.

Fig. 1 shows that the truncated error $e(N)$ in Eq. (15) can be negligible when $N\geqslant\alpha x+4$ holds. Therefore, we can see from Eq. (5) that

$$N\geqslant\max_{i=1,\cdots,C}(2\pi\alpha_i MD/c)+4 \tag{18}$$

must be satisfied.

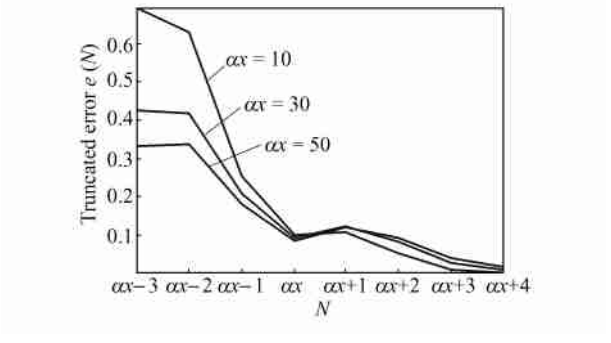


Fig. 1. Truncated error $e(N)$ versus $N$.

If the truncated error $e(N)$ in Eq. (15) can be negligible, the array steering vector can be approximately simplified as

$$\boldsymbol{a}_k(\alpha_i, \theta_k)=\boldsymbol{J}(\alpha_i)\begin{bmatrix} P_0(\sin\theta_k) \\ \vdots \\ P_N(\sin\theta_k) \end{bmatrix}, \tag{19}$$

where

$$\boldsymbol{J}(\alpha_i) \triangleq \begin{bmatrix} \mathrm{j}^0(2\cdot 0+1)j_0(-\alpha_i\cdot 2\pi MD/c) & \cdots & \mathrm{j}^N(2\cdot N+1)j_N(-\alpha_i\cdot 2\pi MD/c) \\ \vdots & \ddots & \vdots \\ \mathrm{j}^0(2\cdot 0+1)j_0(\alpha_i\cdot 2\pi MD/c) & \cdots & \mathrm{j}^N(2\cdot N+1)j_N(\alpha_i\cdot 2\pi MD/c) \end{bmatrix}. \quad (20)$$

Substituting Eqs. (5) and (19) into Eq. (3), the array DOA matrix can be rewritten as

$$\boldsymbol{A}(\alpha_i, \Theta) = \boldsymbol{J}(\alpha_i)\boldsymbol{P}(\Theta), \quad (21)$$

where

$$\boldsymbol{P}(\Theta) = \begin{bmatrix} P_0(\sin\theta_1) & \cdots & P_0(\sin\theta_{d_\alpha}) \\ \vdots & \ddots & \vdots \\ P_N(\sin\theta_1) & \cdots & P_N(\sin\theta_{d_\alpha}) \end{bmatrix}. \quad (22)$$

Given that

$$\boldsymbol{T}(\alpha_i) \triangleq \boldsymbol{J}(\alpha_0)[\boldsymbol{J}^{\mathrm{H}}(\alpha_i)\boldsymbol{J}(\alpha_i)]^{-1}\boldsymbol{J}^{\mathrm{H}}(\alpha_i), \quad i = 1, \cdots, C, \quad (23)$$

we can obtain

$$\boldsymbol{T}(\alpha_i)\boldsymbol{A}(\alpha_i, \Theta) = \boldsymbol{J}(\alpha_0)[\boldsymbol{J}^{\mathrm{H}}(\alpha_i)\boldsymbol{J}(\alpha_i)]^{-1}\boldsymbol{J}^{\mathrm{H}}(\alpha_i)\boldsymbol{A}(\alpha_i, \Theta). \quad (24)$$

Substituting Eq. (21) into Eq. (24), we can obtain

$$\begin{aligned}\boldsymbol{T}(\alpha_i)\boldsymbol{A}(\alpha_i, \Theta) &= \boldsymbol{J}(\alpha_0)[\boldsymbol{J}^{\mathrm{H}}(\alpha_i)\boldsymbol{J}(\alpha_i)]^{-1}\boldsymbol{J}^{\mathrm{H}}(\alpha_i)\boldsymbol{J}(\alpha_i)\boldsymbol{P}(\Theta) \\ &= \boldsymbol{J}(\alpha_0)\boldsymbol{P}(\Theta) = \boldsymbol{A}(\alpha_0, \Theta). \end{aligned} \quad (25)$$

Equations (8) and (25) reveal that $\boldsymbol{T}(\alpha_i)$ defined in Eq. (23) is the focusing matrix, which can change the direction matrix $\boldsymbol{A}(\alpha_i, \Theta)$ into $\boldsymbol{A}(\alpha_0, \Theta)$, where $\alpha_0$ is the reference cycle frequency.

Thus, we can conclude that by utilizing focusing transformation, the source DOAs can be estimated by exploiting the cyclostationary property at multiple cycle frequencies. The algorithm procedure is as follows:

Step 1: For signal $x_i(\cdot)$ received at the $i$th sensor, and for each cycle frequency $\alpha_i$ (estimated or known), estimate the cyclic conjugate correlation function $R_{x_i}^{\alpha_i}(\tau)$, where $\tau = 0, T_s, \cdots, LT_s$; $i = 1, 2, \cdots, 2M+1$; and $T_s$ is the sampling period.

Step 2: For each cycle frequency $\alpha_i$, form the focusing matrix $\boldsymbol{T}(\alpha_i)$ from Eqs. (20) and (23).

Step 3: Form the pseudodata matrix $\boldsymbol{X}$ from Eqs. (11) and (14).

Step 4: Pick the SSF algorithm, e.g. MUSIC or ESPRIT, to estimate the DOAs of SOIs based on the sampling covariance matrix $\overline{\boldsymbol{X}\boldsymbol{X}}^{\mathrm{H}}$.

## 2 Statistical performance analysis

The spectrum function of the MUSIC algorithm is given as

$$\begin{aligned} P_{\mathrm{MUSIC}} &= \Big[a^{\mathrm{H}}(\alpha_0, \theta)\sum_{i=K+1}^{M} e_i e_i^{\mathrm{H}} a(\alpha_0, \theta)\Big]^{-1} \\ &\triangleq [D(\alpha_0, \theta)]^{-1}, \end{aligned} \quad (26)$$

where $\alpha_0 \in \{\alpha_i, i = 1, \cdots, C\}$ and

$$\begin{aligned} D(\alpha, \theta) &= a^{\mathrm{H}}(\alpha_0, \theta)\sum_{i=K+1}^{M} e_i e_i^{\mathrm{H}} a(\alpha_0, \theta) \\ &= 1 - a^{\mathrm{H}}(\alpha_0, \theta)\sum_{i=1}^{K} e_i e_i^{\mathrm{H}} a(\alpha_0, \theta). \end{aligned} \quad (27)$$

It can be seen from Eqs. (11)—(13) that the covariance matrix for the array signal model is

$$\boldsymbol{R} = \sum_{i=1}^{C} \boldsymbol{T}(\alpha_i)\boldsymbol{E}\{\boldsymbol{R}_{\boldsymbol{x}}^{\alpha_i}(\tau)[\boldsymbol{R}_{\boldsymbol{x}}^{\alpha_i}(\tau)]^{\mathrm{H}}\}\boldsymbol{T}^{\mathrm{H}}(\alpha_i), \quad (28)$$

and

$$\mathrm{E}\{\boldsymbol{R}_{\boldsymbol{x}}^{\alpha_i}(\tau)[\boldsymbol{R}_{\boldsymbol{x}}^{\alpha_i}(\tau)]^{\mathrm{H}}\} = \mathrm{A}(\alpha_i)\boldsymbol{R}_{\boldsymbol{s}}(\alpha_i)\boldsymbol{A}^{\mathrm{H}}(\alpha_i) + \sigma_n^2(\alpha_i)I, \quad (29)$$

where

$$\boldsymbol{R}_{\boldsymbol{s}}(\alpha_i) = \mathrm{diag}\{P_k^{\alpha_i}, k = 1, \cdots, K\}. \quad (30)$$

Substituting Eq. (29) into Eq. (28), we have

$$\begin{aligned} \boldsymbol{R} &= \sum_{i=1}^{C} \boldsymbol{T}(\alpha_i)[\boldsymbol{A}(\alpha_i)R_s(\alpha_i)\boldsymbol{A}^{\mathrm{H}}(\alpha_i) + \sigma_n^2(\alpha_i)I]\boldsymbol{T}^{\mathrm{H}}(\alpha_i) \\ &= \sum_{i=1}^{C}[\boldsymbol{T}(\alpha_i)\boldsymbol{A}(\alpha_i)\boldsymbol{R}_{\boldsymbol{s}}(\alpha_i)\boldsymbol{A}^{\mathrm{H}}(\alpha_i)\boldsymbol{T}^{\mathrm{H}}(\alpha_i) + \sigma_n^2(\alpha_i)\boldsymbol{T}(\alpha_i)\boldsymbol{T}^{\mathrm{H}}(\alpha_i)]. \end{aligned} \quad (31)$$

By using Eq. (8), Eq. (31) can be reduced to

$$\begin{aligned} \boldsymbol{R} &= \sum_{i=1}^{C}[\boldsymbol{A}(\alpha_0)\boldsymbol{R}_{\boldsymbol{s}}(\alpha_i)\boldsymbol{A}^{\mathrm{H}}(\alpha_0) + \sigma_n^2(\alpha_i)\boldsymbol{T}(\alpha_i)\boldsymbol{T}^{\mathrm{H}}(\alpha_i)] \\ &= \boldsymbol{A}(\alpha_0)\sum_{i=1}^{C}\boldsymbol{R}_{\boldsymbol{s}}(\alpha_i)\boldsymbol{A}^{\mathrm{H}}(\alpha_0) + \sum_{i=1}^{C}\sigma_n^2(\alpha_i)\boldsymbol{T}(\alpha_i)\boldsymbol{T}^{\mathrm{H}}(\alpha_i). \end{aligned} \quad (32)$$

Substituting Eq. (30) into Eq. (32), it can be seen that

$$\begin{aligned}\boldsymbol{R} &= \sum_{i=1}^{C}[\boldsymbol{A}(\alpha_0)\boldsymbol{R}_s(\alpha_i)\boldsymbol{A}^{\mathrm{H}}(\alpha_0) \\ &\quad + \sigma_n^2(\alpha_i)\boldsymbol{T}(\alpha_i)\boldsymbol{T}^{\mathrm{H}}(\alpha_i)] \\ &= \boldsymbol{A}(\alpha_0)\Omega_s(\alpha_0)\boldsymbol{A}^{\mathrm{H}}(\alpha_0) \\ &\quad + \sum_{i=1}^{C}\sigma_n^2(\alpha_i)\boldsymbol{T}(\alpha_i)\boldsymbol{T}^{\mathrm{H}}(\alpha_i) \\ &\triangleq \boldsymbol{A}(\alpha_0)\Omega_s(\alpha_0)\boldsymbol{A}^{\mathrm{H}}(\alpha_0) + \Omega_n, \end{aligned} \tag{33}$$

where

$$\begin{aligned}\Omega_s(\alpha_0) &= \sum_{i=1}^{C}\mathrm{diag}\{P_k^{\alpha_i}, k = 1, \cdots, K\} \\ &= \mathrm{diag}\left\{\sum_{i=1}^{C}P_k^{\alpha_i}, k = 1, \cdots, K\right\}, \end{aligned} \tag{34}$$

$$\Omega_n = \sum_{i=1}^{C}\sigma_n^2(\alpha_i)\boldsymbol{T}(\alpha_i)\boldsymbol{T}^{\mathrm{H}}(\alpha_i). \tag{35}$$

From Eq. (8), the focusing matrix can also be written as

$$\boldsymbol{T}(\alpha_i) = \boldsymbol{A}(\alpha_0)[\boldsymbol{A}^{\mathrm{H}}(\alpha_i)\boldsymbol{A}(\alpha_i)]^{-1}\boldsymbol{A}^{\mathrm{H}}(\alpha_i). \tag{36}$$

Substituting Eq. (36) into Eq. (35), we have

$$\Omega_n = \boldsymbol{A}(\alpha_0)\left\{\sum_{i=1}^{C}\sigma_n^2(\alpha_i)[\boldsymbol{A}^{\mathrm{H}}(\alpha_i)\boldsymbol{A}(\alpha_i)]^{-1}\right\}\boldsymbol{A}^{\mathrm{H}}(\alpha_0). \tag{37}$$

After singular-value decomposition, $\Omega_n$ becomes

$$\Omega_n = \sum_{k=K+1}^{M}\varepsilon_n^2(\alpha_0)e_k e_k^{\mathrm{H}}. \tag{38}$$

From Eqs. (34) and (38) and according to the deduction procedure in Ref. [9], the estimate accuracy can be obtained

$$\begin{aligned}\mathrm{Cov}\{\alpha_0, \theta_m\} &= \frac{2\varepsilon_n^2(\alpha_0)}{Z\sum_{i=1}^{C}P_m^{\alpha_i}}\left[\mathrm{Re}\left\{\frac{\partial \boldsymbol{a}^{\mathrm{H}}(\alpha_0, \theta_m)}{\partial\theta_m}\Omega_n(\alpha_0)\right.\right. \\ &\quad \left.\left.\circ\frac{\partial \boldsymbol{a}(\alpha_0, \theta_m)}{\partial\theta_m}\right\}\right]^{-1} \\ &\quad + O\left(\varepsilon_n^2(\alpha_0)\Big\backslash\sum_{i=1}^{C}P_m^{\alpha_i}\right). \end{aligned} \tag{39}$$

## 3 Simulation results

In this section, we present the simulation results to demonstrate the effectiveness of our new algorithm. More specifically, we will show that the proposed algorithm can generate a higher resolution than the single-cycle estimator (SC-MUSIC) and conventional spatial spectrum estimation method (Focusing MUSIC).

In the following examples, a thirteen-element uniform linear array was used, with the smallest sensor separation $c/2f_0$ being used to avoid any ambiguity in DOA estimation, where $c$ is the wave speed and $f_0$ is the center frequency with the value of 90 MHz of the effective array manifold. The statistics of the DOA estimates were calculated based on 500 independent trials. The signal-to-noise ratio (SNR) was defined as the ratio of the power of this source to that of the background noise. The background noise is spatially uncorrelated Gaussian noise. For SC-MUSIC algorithm, we evaluated the conjugate cyclic correlation to extract the signal of interest (binary phase-shift keying: BPSK).

### 3.1 Signal selectivity test

The first example was designed to test the signal selectivity of the triple-cycle SC-MUSIC algorithm. Three cycle frequencies were $1/T_c$, $2/T_c$ and $3/T_c$, where $1/T_c$ is the baud rate. The SOI was a BPSK signal with half-cosine pulse shape, 18.75-MHz baud rate ($T_c$=0.053 μs), and 10-dB SNR. It arrived at an angle of 10°. Two interferences QPSK (quarternany phase-shift keying) and BPSK arriving from −10° and 13°, respectively, were also present. The SNRs of QPSK and BPSK were 12 dB and 15 dB, and the baud rates of them were 18.75 MHz and 25 MHz, respectively. 4096 samples were collected at the rate of 60 MHz for 68.27 μs. For simplicity of comparison, we assumed that the cycle frequencies of the signals of interest and the number of sources were known. The DOA estimation result is shown in Fig. 2.

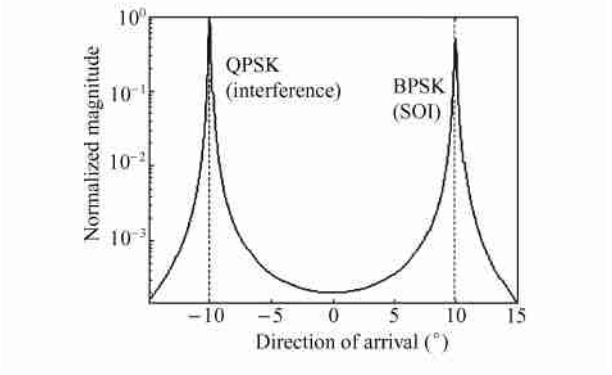


Fig. 2. Result of the triple-cycle SC-MUSIC algorithm.

According to the simulation result in Fig. 2, the triple-cycle SC-MUSIC algorithm reveals two peaks

around $10^{\circ}$ and $-10^{\circ}$. Since the new algorithm exploited the cyclostationary property of the sources, for the cycle frequencies (baud rate = 18.75 MHz), the interfering source (BPSK) with a different cycle frequency (baud rate = 25 MHz) was rejected. Only the sources (SOI and QPSK) with the same cycle frequencies remained.

### 3.2 Revolution test

The results for triple-cycle SC-MUSIC indicate significant improvement in DOA estimation, especially when SNR is low. For example, when SNR is lower than 0dB. Fig. 3 shows that the theoretical estimation accuracy is really close to the simulation accuracy especially when SNR is higher than 0, which can prove the correctness of the statistical performance of the new method.

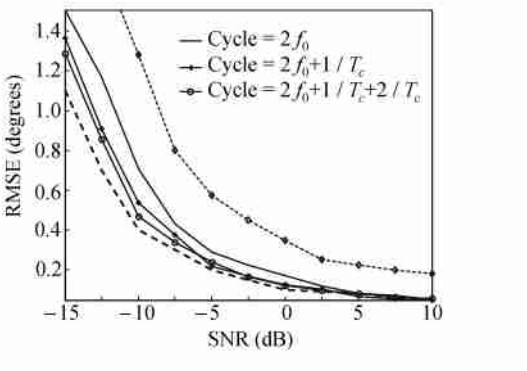


Fig. 3. Results of the single-cycle SC-MUSIC, double-cycle SC-MUSIC and triple-cycle SC-MUSIC algorithms. RMSE: root-mean-square error; cycle = $2f_0$: the single-cycle SC-MUSIC algorithm at the cycle frequency $2f_0$; cycle = $2f_0 + 1/T_c$: the double-cycle SC-MUSIC algorithm at the cycle frequencies $1/T_c$ and $2f_0$; cycle = $2f_0 + 1/T_c + 2/T_c$: the triple-cycle SC-MUSIC algorithm at the cycle frequencies $1/T_c$, $2/T_c$ and $2f_0$; the dashed line: the theoretical root-mean squared error; the dashed line with diamond: the conventional focusing algorithm[10].

It can be seen from Fig. 3 that the double-cycle SC-MUSIC algorithm can produce almost the same result as that of the triple-cycle SC-MUSIC. This is because the cyclostationary properties of the BPSK signal at cycle frequencies other than $2f_0$, $1/T_c$ and $2f_0 \pm 1/T_c$ are not distinct. As for the problem of how to determine the number of the cycle frequencies, it is related to the cyclostationary property of the SOI. Ideally speaking, only when all the cycle frequencies of the SOI are exploited can the multi-cycle SC-MUSIC algorithm perform the best. However, in most cases, some main cycle frequencies are enough for the multi-cycle SC-MUSIC algorithm to obtain satisfactory performance.

## 4 Conclusions

A novel direction-of-arrival approach for wideband cyclostationary signals in this paper has been proposed by exploiting the cyclostationary property at multiple cycle frequencies. Simulation results have demonstrated the effectiveness and superiority of the given methods compared with the existing DOA estimation algorithms.

## References

1 Gardner W. A. Simplification of MUSIC and ESPRIT by exploitation of cyclostationarity. Proc. IEEE, 1988, 76(7): 845—847.
2 Schell S. V. and Gardner W. A. Cyclic MUSIC algorithms for signal-selective direction finding. Proc. ICASSP89 Conf., 1989, 4: 2278—2281.
3 Xu G. H. and Kailath T. Direction-of-arrival estimation via exploitation of cyclostationarity-a combination of temporal and spatial processing. IEEE Trans. Signal Processing, 1992, 40(7): 1775—1785.
4 Xu. G. H. and Kailath T. Array signal processing via exploitation of spectral correlation-A combination of temporal and spatial processing. In: Proc. 23rd Asilomar Conf. Signals, Syst., Comput., Pacific Grove CA, 1989, 11: 945—949.
5 Lee Y. T. and Lee J. H. Direction-finding methods for cyclostationary signals in the presence of coherent sources. IEEE Trans. Antennas and Propagation, 2001, 49(12): 1821—1826.
6 Gardner W. A. Exploiting spectral redundancy in cyclostationary signals. IEEE ASSP Magazine, 1991, 8(2): 14—36.
7 Abhayapala T. D. and Bhatta H. Coherent broadband source localization by modal space processing. In: 10th International Conference on Telecommunications, February 23-march 1, 2003, 190—196.
8 Ghanem R. B. and Frappier C. Spherical Bessel functions and explicit quadrature formula. Mathematics of Computation, 1997, 66(1): 289—296.
9 Kaveh M. and Barabell A. J. The statistical performance of the MUSIC and the minimum-norm algorithms in resolving plane waves in noise. IEEE Trans., 1986, ASSP-34(2): 331—340.
10 Wang H. and Kaven M. Coherent signal-subspace processing for the detection and estimation of angles of arrival of multiple wideband sources. IEEE Trans. ASSP-33, 1985, 33(4): 823—831.